Validation of Finite Element Modelling of Multielectrode Capacitive System for Process Tomography Flow Imaging

S H Khan F Abdullah

Measurement and Instrumentation Centre, Department of EE and Information Engineering, City University, Northampton Square, London EC1V 0HB, UK

ABSTRACT: Finite element modelling of process tomography sensor systems is necessary for their CAD both for performance evaluation and design optimization. This paper involves the validation of finite element models of a 12-electrode capacitive sensor system for multiphase flow imaging. Various results of modelling have been compared in the form of standing mode capacitances and sensor sensitivity distribution with experimental data obtained from UMIST. There is good agreement between simulation results and experiments especially for high sensitivity regions inside the pipe.

1. INTRODUCTION

The area of process tomography flow imaging using capacitive electrode systems is growing rapidly with some promising results obtained already from full scale industrial prototype. The basic principle of flow component detection with capacitive electrodes lies in changes of capacitance values between electrode pairs due to changes in permittivities of flow components. Beck *et al* (1986) proposed to exploit this principle for imaging multiphase flows and the practical implementation of the idea was first made at UMIST by Huang *et al* (1989) who showed the feasibility of an 8-electrode sensor system for imaging two component flows. In such a multielectrode system capacitive electrodes are mounted symmetrically around the flow pipe and all possible independent capacitance measurements are carried out between various electrode pairs by successive electronic interrogation. Comparing to other existing tomography systems, capacitive sensor systems are inexpensive, fast, noninvasive and simple in construction; today various designs of such systems are being explored to be used in diversified industrial applications (Dickin *et al* 1991, Plaskowski *et al* 1991, Hammer *et al* 1991).

Although some of the geometric and physical parameters of capacitive electrode systems are predetermined there is still a number of geometric parameters which are variable and determine the overall performance of the system during exploitation. This obviously necessitates the CAD approach towards understanding, performance evaluation and design optimization of these systems (Khan *et al* 1991). One of the main tasks of CAD of electrode system is the solution of the so called forward problem which involves simulation of electric field distribution inside the flow pipe. This is done by numerical solution of the appropriate Laplace's equation by finite element method (FEM). The data obtained from field simulations and subsequent capacitance calculations, are then used to evaluate system

performance parameters and fed into the solution of the inverse problem of image reconstruction the quality of which reflects the overall system performance. It is, therefore vitally important to ensure the reliability and accuracy of finite element (FE) modelling for CAD and design optimization of such PT sensor systems. The obvious way to do that is to establish confidence on modelling results by comparing them with available experimental data. In the following sections this is done by comparing simulation results with corresponding experimental data obtained at UMIST from various designs of two 12-electrode capacitive systems.

2. FINITE ELEMENT MODEL OF A 12-ELECTRODE CAPACITIVE SYSTEM

The cross section of a 12-electrode capacitive system is shown in Figure 1 which is self explanatory (see also Table 1). Radial screens in between electrodes serve as shields to reduce high capacitance between adjacent electrodes and increase measurement accuracy. The outer screen which is always earthed makes the whole system stray immune. The inner radius R_1 is fixed but the rest of the parameters θ, δ_1, δ_2, scgp, scth and the number of electrodes N are variables which determine system performance. Capacitances between electrode pairs are measured by using special capacitance measuring circuitry developed at UMIST (Huang *et al* 1991). In this one of the electrodes (the 'active electrode') is given a constant potential and the capacitances between this and the rest of the electrodes ('detecting electrodes' kept at virtual earth) are measured. In this way a total of n=N(N-1)/2 independent capacitance measurements can be made by choosing each of the electrodes in turn as active electrodes. The data thus obtained are used to solve the inverse problem of determining flow component distributions in the pipeline cross section and with a suitable image reconstruction algorithm these are visualized on the screen in real time (Xie *et al* 1991). All these could be simulated as a part of CAD before committing to build real systems to predict their performance and optimize geometric parameters.

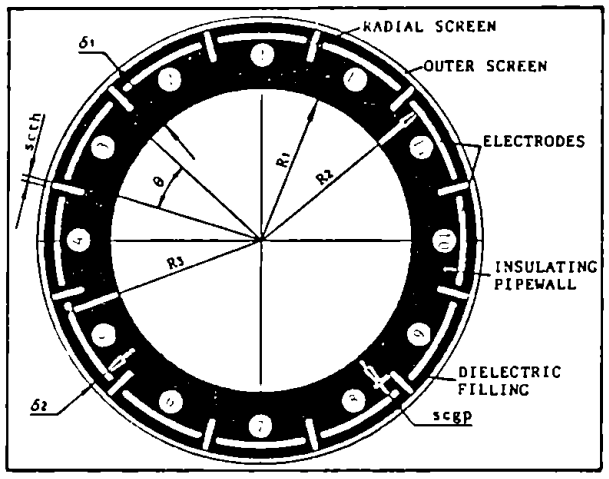

Fig. 1. Cross section of a 12-electrode capacitive system (not in scale)

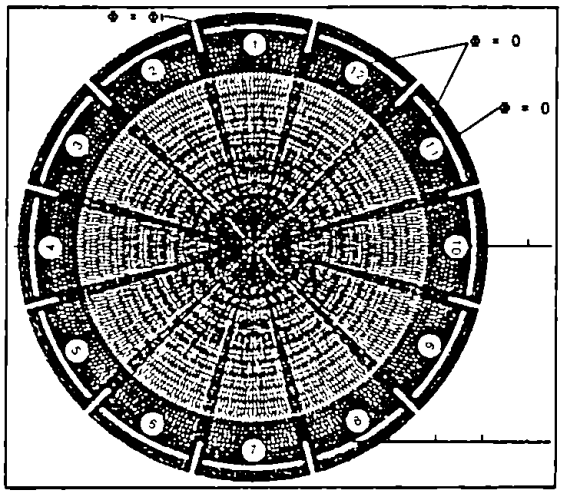

Fig. 2. Finite element model of the 12-electrode capacitive system

By neglecting the fringing field due to finite lengths of electrodes and assuming that flow component distribution remains the same along the length of pipeline within electrode lengths the electric processes in the electrode system shown in Figure 1 can be simulated by the 2D FE model shown in Figure 2. Under appropriate boundary conditions (for example shown in Figure 2), the electrostatic field in the electrode system is calculated

by solving the corresponding Laplace's equation

$$\nabla (\varepsilon(x,y)\ \nabla\Phi(x,y)) = 0 \qquad (1)$$

in terms of the electrostatic potential $\Phi=\Phi(x,y)$ for space-varying permittivities of flow component distributions $\varepsilon=\varepsilon(x,y)$. The solution of this equation under proper boundary conditions by FEM gives potential values at nodal points from which field vectors E, D and subsequently capacitance between any pair of electrodes are calculated.

3. EXPERIMENTAL MODELS OF 12-ELECTRODE CAPACITIVE SYSTEM

Experiments were carried out at UMIST with two different designs of electrode system which have different inner radius R_1 and pipe wall thickness δ_1. All experiments were carried out with and without the presence of interelectrode radial screens to show their effects, quantitatively on various system performance parameters. Figure 3 shows the cross section of one of the two designs of the experimental electrode system without radial screens. In all experimental models the space between the pipe wall outer surface and the outer screen is filled with air and not with dielectric filling material. In course of experiments capacitances were measured between electrode pairs 1-7 and 1-12 when the pipe is empty; these are standing mode capacitances which we represent as C_{017} and C_{0112}

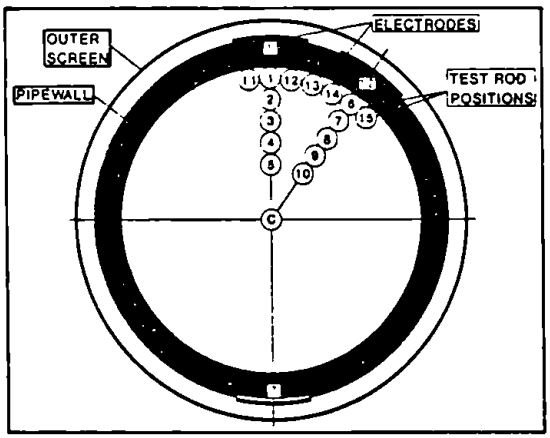

Fig. 3. Cross section of experimental model of the 12 electrode capacitive system showing test rod positions (only three electrodes are shown)

respectively. To explore the sensitivities of various sensor designs a perspex rod of circular cross section is placed axially at different positions inside the pipeline and capacitances between 1-7 and 1-12, C_{17}, C_{112} are measured. These rod positions are represented by numbered circles inside the pipe in Figure 3. The sensitivity (relative) of the system for various test rod positions is expressed as

$$S_{ij} = \Delta C_{ij}/C_{0ij} \qquad (2)$$

where, $\Delta C_{ij} = C_{ij} - C_{0ij}$, C_{ij} - capacitance between electrode pair i-j for a given rod position inside the flow pipe; C_{0ij} - standing mode capacitance between i-j. These data for different test rod positions in various electrode designs are compared with identical data obtained from simulated electrode systems. The following table shows physical and geometric parameters of electrode designs used for experimental and modelling purposes.

Table 1. List of geometric and physical parameters used in experimental and finite element models of 12-electrode capacitive systems

Parameters	Thin pipe wall model		Thick pipe wall model	
	Without radial screen	With radial screen	Without radial screen	With radial screen
1. Pipe inner radius R_1, mm	68	68	78	78
2. Pipe wall thickness δ_1, mm	7	7	12.5	12.5
3. Distance between pipe wall outer surface and outer screen δ_2, mm	6	6	6	6
4. Electrode angle θ, deg.	24	24	25	25
5. Radial screen thickness scth, mm	1.6	1.6	1.6	1.6
6. Electrode thickness elt, mm	0.3	0.3	0.3	0.3
7. Radial screen penetration depth, mm	—	2	—	2
8. Electrode length l, mm	100	100	100	100
9. Relative permittivity of pipewall material ε_{pw}	3	3	3	3
10. Test rod radius R_{rod}, mm	4.5	4.5	4.5	4.5
11. Permittivity of test rod material ε_{rod}	3	3	3	3

4. FINITE ELEMENT REALIZATION OF EXPERIMENTAL MODELS

For all finite element modelling of above electrode systems a powerful 2D electromagnetic software package PE2D (Vector Fields Limited, UK) has been used on Sun Sparcstation 1. Figures 4a (thin pipe wall model without radial screens) and 4b (thick pipe wall model with radial screen) show typical FE models of experimental electrode systems set up by PE2D pre-processor. After discretisation, FE mesh for the model in Figure 4b looks like the one shown in Figure 5. Circular regions inside the pipe in all these models which are marked 1 to 10 and 'C' represent test rod positions corresponding to those shown in Figure 3. Only those regions which are marked are used to simulate test rods during modelling. The rest of the circular regions (unmarked) serve to ensure consistency and symmetry in discretisation pattern. Maximum number of triangular elements used in all models is around 10000 which is the upper limit for the version of PE2D (version 8.1) used for modelling purposes.

As can be seen from Figure 1 the geometry of the electrode system with curved electrodes, radial screens, etc. is fairly complicated to set up FE models like those shown in Figure 4 quickly and accurately. With the addition of circular regions for test rods setting up of models gets even more complicated. To tackle this a systematic approach is taken at the pre-processing stage in which all models are built up from basic 'building

blocks' like the one shown in Figure 6. This group of regions is then copied to other quadrants by successive mirror reflections to get the full model (shown, for example in Figure 4b). To build this basic block all regions outside the inside of the pipe are first drawn in which the presence or the absence of radial screens is incorporated (Figure 7). The next stage is to draw holes at rod positions inside the pipe by using

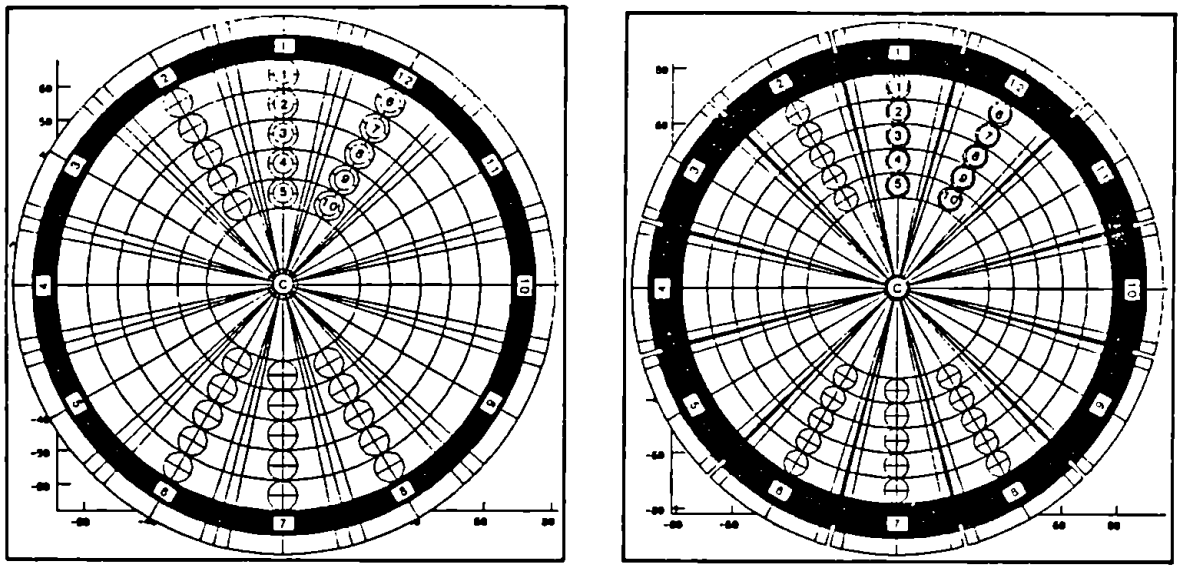

a) b)

Fig. 4. Finite element models of experimental electrode systems a) thin pipe wall model without radial screen b) thick pipe wall model with radial screen

suitably placed curvilinear quadrilateral regions shown in Figure 8. Circular regions for test rods are then drawn in local coordinate systems at rod positions by replicating respective annular regions (Figure 6). All

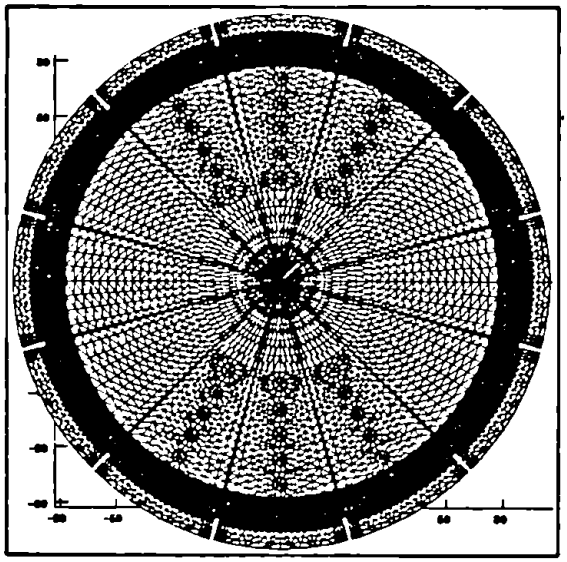

Fig. 5. FE mesh corresponding to electrode system in Fig 4b

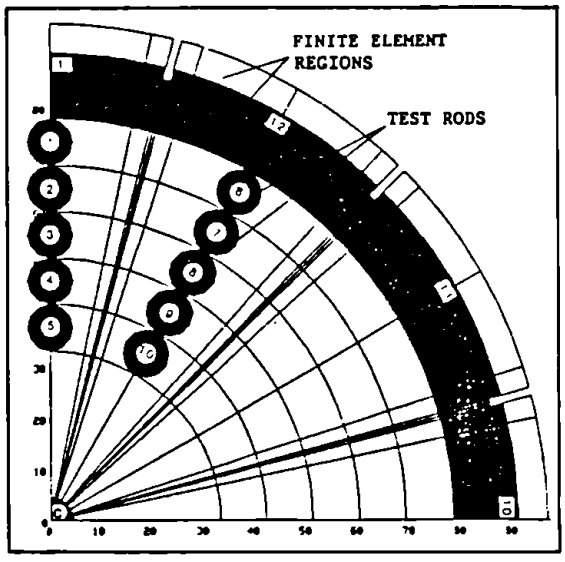

Fig. 6. The basic 'building block' used to set up FE models

these regions are initially assigned the relative permittivity of vacuum (ε=1) which enables the modelling of electrode systems with empty pipes. To

simulate the electrode system with the test rod placed at one of the positions the permittivity of the corresponding circular region in the model is modified to that of the test rod as shown in Figure 9 where the test rod is placed at rod position 2 between electrodes 1 and 7. In this way the experimental designs of the 12-electrode system are simulated for different positions of test rod placements (positions 1 to 10 and 'C' in Figures 4a and 4b). Using PE2D's pre-processing facilities all necessary commands for above operations are written once and stored in files which can be easily and quickly modified and called upon to have them automatically executed to set up models, solve equations and do necessary post-processing for output data.

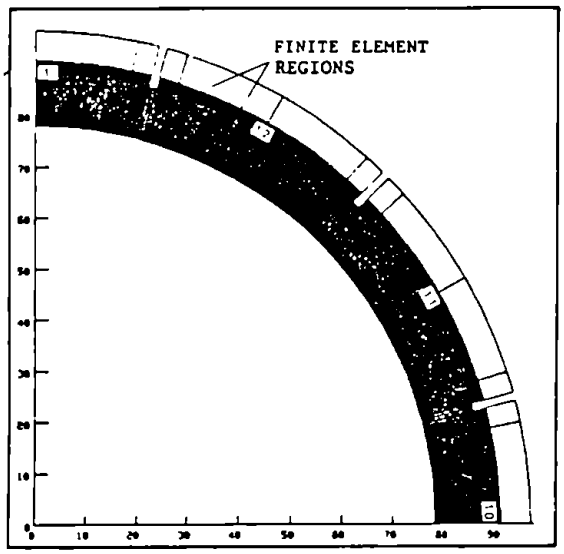

Fig. 7. First stage in building up of the basic 'building block'

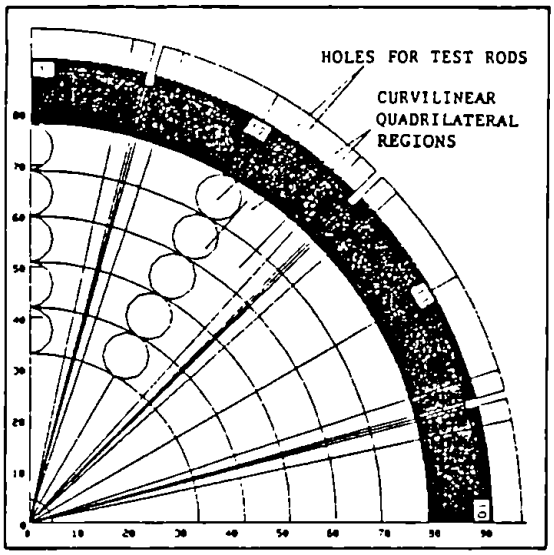

Fig. 8. Final stage in building up of the basic 'building block'

For all FE models equation (1) is solved for electrode 1 selected as the active electrode. A constant electric potential of 1 V is given to this active electrode and rest of the electrodes as well as outer and radial

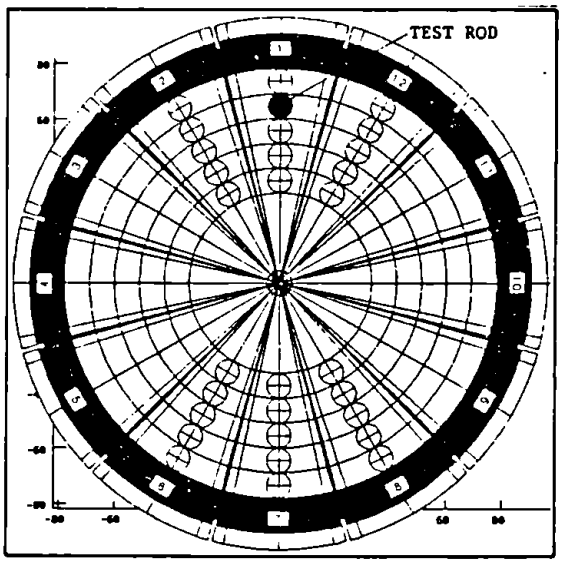

Fig. 9. Positioning of the simulated test rod in FE models

screens are kept at zero potential. Capacitances C_{17} and C_{112} are calculated between electrode pairs 1-7 and 1-12 by determining the total charge Q distributed on electrodes 7 and 12 using $Q=\epsilon\int_s \mathbf{E}.d\mathbf{s}$ (Gauss's Law).

5. MODELLING RESULTS - COMPARISON WITH EXPERIMENTAL DATA AND DISCUSSIONS

Table 2 below shows standing mode capacitances C_{017} and C_{0112} obtained from simulations and experiments. These results confirm quantitatively the effects of interelectrode radial screens and pipe wall thickness on standing mode capacitances between electrode pairs. Since sensitivity requirements of capacitance measuring circuitry depend largely on minimum values of standing mode capacitances for a given sensor geometry it is important to be able to predict these values beforehand by simulations. It is equally useful to predict and determine the pattern of these capacitance changes for a possible variation of key sensor geometric parameters like R_1, δ_1 and scgp. As can be seen from Table 2 increases in δ_1 and R_1 lead to increases in values of both C_{017} and C_{0112}. For C_{017} it is due to

Table 2. Comparison between standing mode capacitances obtained from experimental and simulation models

Capacitances		Thin pipe wall model (R_1=68 mm, δ_1=7 mm)		Thick pipe wall model (R_1=78 mm, δ_1=12.5 mm)	
		No radial screen scgp=0	With radial screen scgp=2	No radial screen scgp=0	With radial screen scgp=2
C_{017} (pF)	Experimental	0.0124	0.011	0.013	0.0115
	Simulated	0.0172	0.0118	0.0176	0.0127
	Deviation (%)	38.70	7.27	35.38	10.43
C_{0112} (pF)	Experimental	1.217	0.424	1.493	0.618
	Simulated	1.306	0.489	1.568	0.726
	Deviation (%)	7.31	15.33	5.02	17.47

combined effects of increased electrode widths (defined by θ) and the distance between them; for C_{0112} increases in higher permittivity material between electrode pair 1-12 and electrode widths lead to increase in capacitances between them. As said earlier, radial screens are meant for reducing high capacitances between adjacent electrodes and this can be seen quantitatively from C_{0112} values obtained by simulations and experiments for electrode models with and without radial screens. At the same time presence of radial screens reduces slightly the standing mode capacitances between distant electrodes, say C_{017} which can be explained by the deviation of field lines away from those electrodes towards closer radial screens which have the same zero potential as distant electrodes.

Comparison between capacitance values shown in Table 2 shows that maximum deviation (38.7%) of simulation results from experimental ones is obtained for capacitances C_{017} the values of which far exceed corresponding values

of capacitances C0112 for which a minimum deviation of around 5% is obtained. These differences between simulated and experimental results could be explained by combined effects of possible experimental and modelling errors discussed later in this section.

Variations of sensitivities (determined by equation (2)) of various sensor models for different test rod positions are shown in Figures 10 and 11 in which numbers 1 to 10 and 'C' along x-axis represent test rod positions corresponding to those in Figure 4. Both simulation and experimental results in Figures 10 and 11 clearly reflect the effects of pipe wall thickness δ_1 and radial screens (radial screen penetration depth scgp) on sensor sensitivity distributions inside the pipe. For various rod positions in between electrodes 1 and 7 presence of radial screens increases (15-25%) sensitivities S_{17} when δ_1=const. Pipe wall thickness δ_1 shows to have higher effects on sensitivity distributions S_{17} than radial screens. Figure 10 shows that for an about 80% increase in δ_1 sensitivities S_{17} decrease upto 100% (scgp=const.). All these patterns of sensitivity variations could also be seen in Figure 11 in respect of sensitivities S_{112} between

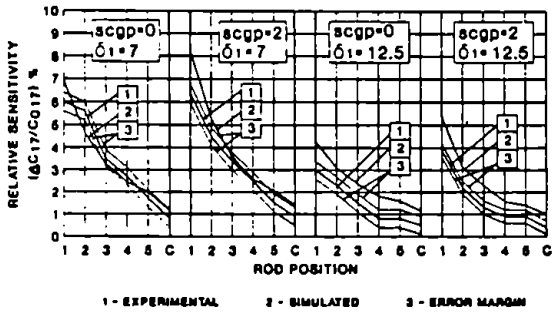

Fig. 10. Variation of relative sensitivity S_{17} with test rod position

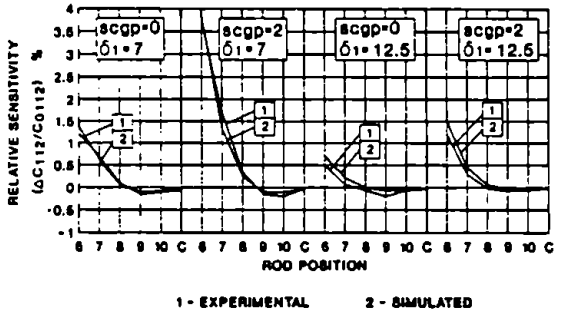

Fig. 11. Variation of relative sensitivity S_{112} with test rod position

electrodes 1-12. For test rod positions 6 and 7 high increase in sensitivity is observed in presence of radial screens which is most probably due to diversions of field lines, going towards electrode 12 through high permittivity test rod at positions 6 and 7. On the other hand the presence of test rods at positions 8-10 and at the centre 'C' diverts field lines away from electrode 12 resulting in very small or negative sensitivities S_{112} between electrodes 1 and 12. As in the case of S_{17} increase in pipe wall thickness δ_1 also reduces sensitivities S_{112} for a given scgp=const. This is because more and more field lines tend to go through increased pipe wall material towards electrode 12 without penetrating into the pipeline. An extreme case for this would be the sensitivity S_{112}=0 for the test rod placed at position 6 in an electrode system with extremely high δ_1.

By comparing experimental and simulated sensitivity variation curves in Figures 10 and 11 it can be concluded that deviations of simulation results from experimental ones vary differently for different sensitivities and electrode designs. Although there is no apparent consistent pattern of this variation what is evident from these figures is the occurrence of maximum deviations for low sensitivity regions between electrodes 1-7 and 1-12. While simulation results for sensitivities S_{17} (Figure 10) are showing reasonable agreement (considering, especially experimental error margins (3)) with experimental ones some high disagreements are observed for negative sensitivities S_{112} (Figure 11). This is particularly true for test rod at positions 9-10 and 'C' for which very low values of capacitance

change ΔC_{112} are obtained.

The above disagreements between experimental and simulation results could be explained by analyzing various errors associated with both modelling and experiments. The main sources of experimental errors could be: baseline drift of sensor electronic circuit, noise voltage generated in it, geometry of electrode designs used, inaccurate positioning of test rods, etc. Discretisation errors and errors in capacitance calculations could be considered as two main sources of errors during numerical modelling.

The baseline drift of sensor electronic circuit which is caused mainly by its temperature dependency could lead to errors in capacitance measurements, especially when the circuit is switched on for a long time during experiments and temperature changes take place in between capacitance measurements for various test rod positions. For a temperature change of 10^0 C the effect of baseline drift could be comparable to an input capacitance change of 5 fF (Huang *et al* 1991) which is significantly higher than most capacitance changes ΔC_{ij} caused by various test rod positions during experiments. This obviously could lead to uncertainties in sensitivity values calculated from measured capacitances, especially for low sensitivity areas in between electrodes 1-7 and 1-12 inside the pipeline. The sensor electronics used at the time of above experimental studies was not baseline drift corrected and all measures were taken to reduce its effects below 0.1fF. At present, the sensor electronics provided with 12-electrode sensor systems are self-baseline drift corrected which eliminates above measurement errors (Huang *et al* 1991).

The capacitance measuring circuit used for sensor electrodes measures capacitances as dc voltage signals from detecting electrodes which are proportional to unknown capacitances. That is why it is important to know the level of noise voltage generated in the circuit as it contributes to errors in capacitance measurements. By taking different preventive measures to eliminate various sources of noise voltages a rms noise level of 0.07 fF could be achieved (Huang *et al* 1991) which is quite low comparing to measurement resolution of the circuit (0.3 fF) but comparable to some of the ΔC_{ij} obtained in experiments.

Variations in geometric features of electrode systems could be considered as potential sources of errors in measured capacitance values obtained during experiments. As can be seen from Table 1 experiments are carried out in two different models of sensor electrodes - thin pipe wall model and thick pipe wall model. It can be assumed that there are technological errors in making those models which contribute to uncertainties in their precise geometric specifications, for example precise positioning of capacitive electrodes and radial screens, concentricity of outer screen, etc. All these give inaccuracies in experimental results and lead to uncertainties in comparability of results from various models and methods of studies of sensor electrodes - experimental and numerical. For example, simulation results show that both capacitances C_{17} and C_{112} change with the variation of outer screen distance δ_2 from electrodes (Khan *et al* 1991). For a 12-electrode system standing mode capacitances C_{017} and C_{0112} could increase upto 0.4 fF and 0.05-0.09 pF respectively for each mm increase in δ_2 which are comparable and sometimes significantly higher (in case of C_{0112}) than most of the values of ΔC_{ij} obtained from experiments.

Inaccurate positioning of test rod at given positions inside the pipeline

during experiments could be considered as one of the main causes of disagreements between experimental and simulation results, especially for test rod positions in regions of high sensitivity. While in numerical modelling simulated test rods could be placed almost exactly at positions (1-10 and 'C') shown in Figures 3 and 4 it is far more difficult to do that in experimental models. For experimental results shown in Figures 10 and 11 inaccuracies in the positioning of the test rod at various positions are considered to be ±3 mm. The effects of these 'positioning errors' on sensitivity variation curves could be roughly estimated from gradient of these experimental curves shown in Figures 10 and 11. For example +3 mm positioning error at test rod position 2 (model with δ_1=7 mm and scgp=0 in Figure 10) would give an error of 13% in sensitivity (S_{17}) calculations; for position 6 (model with δ_1=12.5 mm and scgp=2 mm) in Figure 11 this would reach upto 25% for sensitivity S_{112}. Higher gradients of sensitivity variation curves for test rods at high sensitivity regions inside the pipe show that positioning errors are higher in those regions.

Errors associated with numerical modelling are usually inherent to the particular modelling method and package used and with correct modelling strategy they could be minimized to get required accuracy. As said earlier, two main sources of modelling errors in the simulation of sensor electrodes by FEM are finite element discretisation and capacitance calculations from field solutions. Discretisation errors are minimized by proper and adequate refining of FE mesh. Any discretisation error which cannot be corrected by further mesh refinement is maintained consistent for various models to ensure comparability of simulation results. For results shown in Figures 10 and 11 FE meshes for all models have been adequately refined to minimize discretisation errors. To show this adequacy simulation results from full models (Figures 4a and 4b) have been compared with those from half models (with twice finer mesh for the same number of FE triangles as in full models) which shows, for example that for the thick pipe wall model (δ_1=12.5 mm, scgp=0) the difference in calculated capacitances C_{017} obtained from full and half models is only 1.3%. In terms of sensitivity this gives a deviation of less than 1% for test rod at position 1.

Errors in capacitance calculations from field solutions are usually associated with numerical integration by which total charge distributed on detecting electrodes is calculated (section 4). Using PE2D's post-processing features these errors could be reduced to an insignificant value by selecting suitable tolerance factor in line integration.

6. CONCLUSIONS

In light of above discussions, simulation and experimental results produced in Table 2 and Figures 10 and 11 it can be concluded that numerical simulation of capacitive electrode systems by FEM could be used confidently to design these systems, predict and evaluate performances at various stages of their CAD.

7. ACKNOWLEDGEMENTS

The authors would like to thank SERC for financial support and professor M. S. Beck and his Group at UMIST, especially Dr. S. M. Huang (now with Schlumberger Cambridge Research Limited, UK) for providing us with experimental data and Dr. C. G. Xie for valuable suggestions and discussions at various stages of the work.

9. REFERENCES

Beck M S, Plaskowski A and Green R G 1986 *Proceedings of the 4th International Symposium on Flow Visualization, 26 - 28 August 1986* (Hemisphere Publishing Corporation) pp 585 - 588

Dickin F G, Hoyle B S, Hunt A, Huang S M, Illyas O, Lenn C, Waterfall R, Williams R A, Xie C G and Beck M S 1991 *Sensors: Technology, Systems and Applications* ed K T V Grattan (Bristol: Adam Hilger) pp 191-196

Hammer E A and Nordtvedt J E 1991 *Sensors: Technology, Systems and Applications* ed K T V Grattan (Bristol: Adam Hilger) pp 233-238

Huang S M, Plaskowski A B, Xie C G and Beck M S 1989 *J. Phys. E, Sci. Instrum.* 22 pp 173 - 177

Huang S M, Xie C G, Thorn R, Snowden D and Beck M S 1991 *Sensors: Technology, Systems and Applications* ed K T V Grattan (Bristol: Adam Hilger) pp 197-202

Khan S H and Abdullah F 1991 *Sensors: Technology, Systems and Applications* ed K T V Grattan (Bristol: Adam Hilger) pp 209-214

Plaskowski A, Bukalski P, Habdas T and Skolimowski J 1991 *Sensors: Technology, Systems and Applications* ed K T V Grattan (Bristol: Adam Hilger) pp 221-226

Xie C G, Plaskowski A and Beck M S 1989 *IEE Proc.* 136 (4) pp 173 - 183

Xie C G, Stott A L, Plaskowski A and Beck M S 1990 *Meas. Sci. Technol.* 1 pp 65 - 78

Xie C G, Huang S M, Hoyle B S and Beck M S 1991 *Sensors: Technology, Systems and Applications* ed K T V Grattan (Bristol: Adam Hilger) pp 203-208